BINARY GMSK: CHARACTERISTICS AND PERFORMANCE

Kuang Tsai and Gee L. Lui
The Aerospace Corporation, El Segundo, California

ABSTRACT

Gaussian Minimum Shift Keying (GMSK) is a form of Continuous Phase Modulation (CPM) whose spectral occupancy can be easily tailored to the available channel bandwidth by a suitable choice of signal parameters. The constant envelope of the GMSK signal enables it to corporate with saturated power amplifier without the spectral re-growth problem. This paper provides a quantitative synopsis of binary GMSK signals in terms of their bandwidth occupancy and coherent demodulation performance. A detailed account of how to demodulate such signals using the Viterbi Algorithm (VA) is given, along with analytical power spectral density (PSD) and computer simulated bit-error-rate (BER) results for various signal BT products. The effect of adjacent channel interference (ACI) is also quantified. Ideal synchronization for both symbol time and carrier phase is assumed.

KEY WORDS

CPM, PAM Representation, GMSK, Bandwidth Efficient Modulation, Pre-coding, Viterbi Algorithm.

1. INTRODUCTION

Gaussian Minimum Shift Keying (GMSK) is a form of Continuous Phase Modulation (CPM) whose spectral occupancy can be easily tailored to the available bandwidth by suitable choice of signal parameters. The signal also bears constant envelope, thus enabling it to avoid the typical spectral re-growth associated with non-linear power amplifiers. These attributes render GMSK an attractive modulation waveform in all Frequency Division Multiple Access (FDMA) communication systems with constrained system bandwidth.

In a paper by Kaleh[1], a simple coherent receiver for binary GMSK was proposed. The receiver is based on a Pulse Amplitude Modulation (PAM) representation of binary CPM signals established by Laurent[2], and employs the Viterbi Algorithm (VA) to optimally demodulate the symbol sequences. This PAM-based receiver offers an effective way of trading receiver performance and complexity by way of varying the number of matched-

filters used. In particular it was shown that, for binary GMSK with BT=1/4 and channel BER≥0.01, a receiver consisting of only two matched-filters and a 4-state VA can virtually achieve the performance of coherent BPSK signaling. The purpose of this paper is to detail the VA-related processing that underlies this PAM-based receiver, and to report further performance results for GMSK signals with other BT values – in particular BT=1/5. Perfect synchronization in both symbol time and carrier phase is assumed throughout this paper – receiver performance with timing and phase tracking is treated in later papers of this session.

Section 2 defines the GMSK signal and assesses its spectral occupancy following a concise review of Laurent's PAM representation of binary CPM signal. Section 3 introduces a data pre-coding scheme and provides a detailed account of how to coherently demodulate a binary GMSK signal using the Viterbi algorithm. Section 4 contains BER simulation results quantifying the performance of the PAM-based coherent receiver for GMSK signal with various BT values.

2. SIGNAL REPRESENTATION AND SPECTRAL OCCUPANCY

A binary GMSK signal $s(t)=\mathrm{Re}\{z(t)\cdot\exp[j\cdot 2\pi f_c t]\}$ at carrier f_c is defined by its complex envelope

$$z(t)=\sqrt{2E_s/T_s}\cdot\exp\{j\cdot[f(t)+f_c]\} \tag{1}$$

where E_s is the bit energy, T_s is the bit duration, f_c is the fixed carrier phase and

$$f(t)=ph\sum\nolimits_n a_n\cdot g(t-nT_s) \tag{2}$$

is the data-modulated phase. Here, h is the modulation index, $a_n\in\{\pm 1\}$ are equally probable NRZ data symbols, and $g(t)$ is the so-called GMSK *phase pulse* which is derived from the GMSK *frequency pulse* $f(t)$ via $g(t)=\int_{(-\infty,\,t)} f(t)dt$. The frequency pulse $f(t)$ is obtained by taking the (non-causal) pulse response of a Gaussian smoothing filter with (single-sided 3-dB) bandwidth B, truncating it to the interval $[-LT_s/2,\,+LT_s/2]$ of duration LT_s, and then right-shifting it by $LT_s/2$ to achieve the required conditions $g(0)=0$ and $g(LT_s)=1$. For Gaussian filters with small BT-product, L is essentially given by $L=1/BT_s$; for BT-product nearing unity, one can still take L as $1/BT_s$ since the conditions $g(0)=0$ and $g(LT_s)=1$ can always be forged by properly scaling the truncated pulse response $f(t)$. For a Gaussian filter with bandwidth B and truncation width $LT_s=1/B$, the GMSK phase pulse $g(t)$ can be directly computed from

$$g(t)=1+\frac{1}{T_s}\left\{t_1Q(st_1)-t_2Q(st_2)-\frac{1}{s\sqrt{2p}}\left[e^{-(st_1)^2/2}-e^{-(st_2)^2/2}\right]\right\} \tag{3}$$

$$t_1=t-(L+1)T_s/2,\quad t_2=t-(L-1)T_s/2,\quad s=2pB/\sqrt{\ln 2}$$

via $Q(x)\equiv\int_{(x,\,\infty)}(1/\sqrt{(2\pi)})\cdot\exp(-y^2/2)dy$. By virtue of (2), the integer L is the number of elapsed bit periods for the GMSK signal to accrue a complete phase change amount of pha due to a single input bit a, and hence represents the memory of the GMSK signal. A

GMSK signal with memory $L>1$ is termed *partial response* GMSK, otherwise it is termed *full response* GMSK.

For any N-bit long binary data sequence $\{a_n;\ 0\le n<N\}$, the complex envelope $z(t)$ of GMSK signal (setting $f_c=0$ for perfect synchronization) takes on the following PAM form[2]

$$z(t) = \sqrt{2E_s/T_s}\cdot\sum_{k=0}^{Q-1}\sum_{n=0}^{N-1} a_{k,n}\cdot h_k(t-nT_s) \tag{4}$$

where $Q=2^{L-1}$ is the total number of PAM-pulses $\{h_k(t)\}$, and $\{a_{k,n}\}$ are the "pseudo-symbols" relating to the channel symbols $\{a_n\}$ via the radix-2 digits $\{k_i\}$ of k (defined as $k=\sum_{i=1}^{L-1}k_i\cdot 2^{i-1}$ with $k_0=0$):

$$a_{k,n} = \exp\left[jph\cdot\left(\sum_{m=0}^{n} a_m - \sum_{i=0}^{L-1} k_i\cdot a_{n-i}\right)\right] \tag{5}$$

Each of the PAM-pulses $h_k(t)$ is completely determined – via a *generalized phase pulse* $c(t)$ – by the modulation index h, the truncation width LT_s, and the underlying GMSK phase pulse $g(t)$:

$$h_k(t) = \prod_{i=0}^{L-1} c\left(t+iT_s-(1-k_i)LT_s\right) \tag{6}$$

$$c(t) = \begin{cases} \sin[ph - phg(|t|)]/\sin(ph), & |t|\le LT_s \\ 0 & |t|\ge LT_s \end{cases} \tag{7}$$

and is time-limited to the interval $[0,\ D_kT_s]$ where $D_k=min_{0\le i<L}\{L(2-k_i)-i\}$, e.g., $D_0=L+1$, $D_1=L-1$.

Spectral occupancy of binary GMSK signals can be analytically assessed by taking the GMSK phase pulse in (3) and effecting the algorithm[3] that computes the analytical PSD $S(f)$ of general CPM signals. In particular, for equally probable channel symbols and non-integer modulation index h, the analytical PSD $S(f)$ can be directly computed from

$$S(f) = 2\cdot\left\{\begin{aligned}&\int_0^{LT_s} R(t)\cos(2pft)dt + \left[\frac{1-C\cos(2pfT_s)}{1+C^2-2C\cos(2pfT_s)}\right]\cdot\int_{LT_s}^{LT_s+T_s} R(t)\cos(2pft)dt \\ &\qquad -\left[\frac{C\sin(2pfT_s)}{1+C^2-2C\cos(2pfT_s)}\right]\cdot\int_{LT_s}^{LT_s+T_s} R(t)\sin(2pft)dt\end{aligned}\right\} \tag{8}$$

$$R(t) = \left(\frac{1}{T_s}\right)\cdot\int_0^{T_s}\prod_{i=-(L-1)}^{ceil(t/T_s)}\left\{\frac{1}{2}\cdot\frac{\sin\{2ph[g(t+t-iT_s)-g(t-iT_s)]\}}{\sin\{ph[g(t+t-iT_s)-g(t-iT_s)]\}}\right\}dt\ ,\qquad C=\frac{1}{2}\cdot\frac{\sin(2ph)}{\sin(ph)}$$

As shown in Figure 1, which contains normalized PSD [i.e., $S(f)/S(0)$] for binary GMSK signals with $h=1/2$, both the mainlobe width and the sidelobe level of the GMSK spectrum decrease with decreasing BT-product. [In general, lowering the modulation index h while keeping the BT-product constant will further reduce the spectral occupancy. In this paper, however, the constraint $h=1/2$ is imposed as a sufficient condition for the data pre-coding scheme described below.]

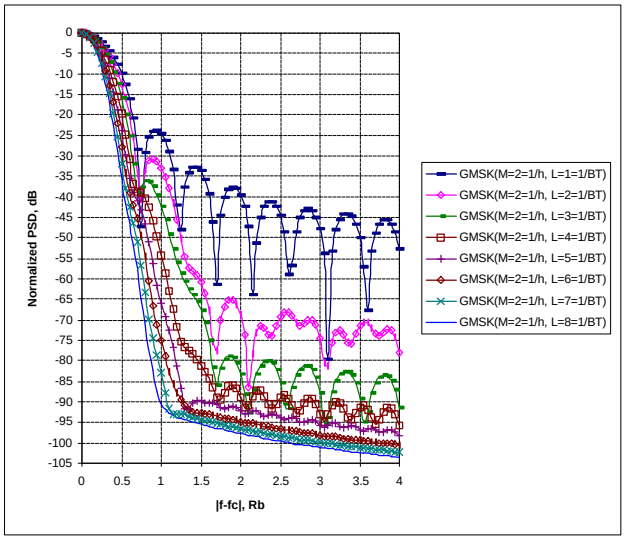

Figure 1. Normalized PSD for Binary GMSK (h=1/2).

The corresponding in-band power ratios (shown in Figure 2) indicate that GMSK signals with smaller BT-products require a narrower band around the carrier to achieve a fixed in-band power ratio. Table A summarizes the spectral occupancy of binary GMSK signals with h=1/2 in terms of their (single-sided) "60-dB bandwidth" and "0.99-power bandwidth" in units of bit rate R_b.

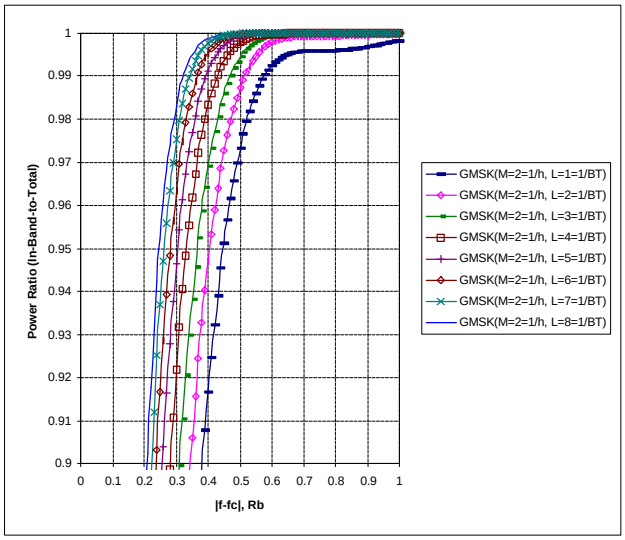

Figure 2. In-band Power Ratio for Binary GMSK (h=1/2).

BT	60-dB Bandwidth (R_b)	0.99-Power Bandwidth (R_b)
1	1.70	0.58
1/2	1.48	0.52
1/3	1.27	0.47
1/4	1.06	0.43
1/5	0.94	0.40
1/6	0.83	0.37
1/7	0.77	0.35
1/8	0.72	0.33

Table A. Single-sided Spectral Occupancy for Binary GMSK (h=1/2).

3. DATA PRE-CODING AND TRELLIS DEMODULATOR

The optimal demodulator for an N-bit waveform $\{a_n;\ 0\le n<N\}$ corrupted by additive white Gaussian noise (AWGN) is one that maximizes the following 2^N correlation metrics ($0\le m<2^N$)

$$\Lambda^{(m)} = \mathrm{Re}\left[\langle z_r(t), z_m(t)\rangle\right] \equiv \mathrm{Re}\left[\int_{-\infty}^{\infty} z_r(t)\cdot z_m^{\,*}(t)dt\right]$$

where $z_m(t)$ denotes the signal associated with the m-th possible data sequence, and $z_r(t)$ denotes the AWGN-corrupted received signal. Expressing $z_m(t)$ in PAM form (4), these metrics become[1]

$$\Lambda^{(m)} = \sqrt{2E_s/T_s}\sum_{n=0}^{N-1} l^{(m)}(n)$$

$$l^{(m)}(n) \equiv \mathrm{Re}\left[\sum_{k=0}^{Q-1} r_{k,n}\cdot a_{k,n}^{(m)*}\right] \tag{9}$$

$$r_{k,n} \equiv \int_{-\infty}^{\infty} z_r(t)\cdot h_k(t-nT_s)dt = \left[z_r(t) * h_k(-t)\right]_{t=nT_s} \tag{10}$$

with $a_{k,n}^{(m)}$ denoting the pseudo-symbols associated with the m-th data sequence. By applying the matched-filter output $r_{k,n}$ ($0\le k<Q$) to a Viterbi algorithm, which recursively selects an optimal pseudo-symbol sequence $\{a_{0,n};\ 0\le n<N\}$ that maximizes Λ, the data sequence $\{a_n\}$ can be effectively demodulated using (5). This PAM-based trellis demodulator is simplified by retaining only the first F matched-filters $\{h_k(-t);\ 0\le k<F\}$ in (9); F is often confined to powers of two due to the "batch" nature of $\{D_k\}$, e.g., D_2=D_3=L-2, D_4=D_5=D_6=D_7=L-3. Of particular interest is the case of F=2, with the corresponding matched-filters (6) and branch metric (9) equations given by

$$h_0(t) = \prod_{i=1}^{L} c(t-iT_s), \qquad h_1(t) = h_0(t)\cdot\frac{c(t+T_s)}{c(t-(L-1)T_s)}$$

$$l(n) \equiv \mathrm{Re}\left[r_{0,n}\cdot a_{0,n}^{*} + r_{1,n}\cdot a_{1,n}^{*}\right] \tag{11}$$

By virtue of the PAM representation, in particular (5), the optimal pseudo-symbol sequence produced by the trellis demodulator at any stage n inevitably involves all the data symbols prior to that stage:

$$a_{0,n} = J^{(a_0+a_1+\cdots+a_n)}, \quad a_{1,n} = J^{a_n} \cdot a_{0,n-2} \tag{12}$$

where $J \equiv \exp(j\pi h) = j$ for $h=1/2$. This intrinsic data dependency calls for a "differential decode" operation when it comes to demodulating the actual data symbols (i.e., $ja_n = a_{0,n} \cdot a^*_{0,n-1}$), thus resulting in a "differential" BER degradation similar to that of DPSK as compared to BPSK. The purpose of the data pre-coding scheme is to encode the source symbols $\{d_n = \pm 1\}$ prior to the GMSK modulation so that the resulting channel symbols $\{a_n\}$ will render an optimal pseudo-symbol sequence requiring no differential decode, hence improving the receiver performance. This can be achieved for binary GMSK with $h=1/2$:

$$a_n = d_n \cdot d_{n-1} = [d_n - d_{n-1} + 1]_{\text{mod } 4} \quad (a_0 = d_0) \tag{13}$$

This pre-coding scheme preserves the transmit spectrum of the GMSK signal because the pre-coded symbols $\{a_n\}$ are still equally probable as the source symbols $\{d_n\}$. With the data pre-code (13) in place, the optimal pseudo-symbol sequence produced by the trellis demodulator becomes, as opposed to (12),

$$a_{0,n} = J^n \cdot J^{d_n} = j^{n+1} \cdot d_n, \qquad a_{1,n} = J^{n-1} \cdot J^{d_n - d_{n-1} + d_{n-2}} = j^n \cdot d_n d_{n-1} d_{n-2} \tag{14}$$

Here we see that, with the state defined as $s_n = (d_n, d_{n-1})$, a 2^2-state 2^3-branch Viterbi algorithm is sufficient for demodulating $\{d_n\}$ using $F=2$ matched-filters. [For each of the 2^2 states $s_n = (d_n, d_{n-1})$ at stage n, there are only two incoming branches from the "previous stage" $s_{n-1} = (d_{n-1}, d_{n-2}) = (d_{n-1}, \pm 1)$.] The corresponding branch metric (11) becomes

$$l(n) = l(s_n, s_{n-1}) = \begin{cases} +\text{Im}(r_{0,n}) \cdot d_n + \text{Re}(r_{1,n}) \cdot d_n d_{n-1} d_{n-2}; & n \equiv 0 \mod 4 \\ -\text{Re}(r_{0,n}) \cdot d_n + \text{Im}(r_{1,n}) \cdot d_n d_{n-1} d_{n-2}; & n \equiv 1 \mod 4 \\ -\text{Im}(r_{0,n}) \cdot d_n - \text{Re}(r_{1,n}) \cdot d_n d_{n-1} d_{n-2}; & n \equiv 2 \mod 4 \\ +\text{Re}(r_{0,n}) \cdot d_n - \text{Im}(r_{1,n}) \cdot d_n d_{n-1} d_{n-2}; & n \equiv 3 \mod 4 \end{cases} \tag{15}$$

A slightly different data pre-coding scheme is also possible for binary GMSK with $h=1/2$:

$$a_n = (-1)^n \cdot d_n \cdot d_{n-1} = (-1)^n \cdot [d_n - d_{n-1} + 1]_{\text{mod } 4} \quad (a_0 = d_0) \tag{16}$$

The pre-coding scheme (16), being a "sign-alternating" variant of that in (13), also preserves the transmit spectrum of the GMSK signal. With the sign-alternating data pre-code (16) in place, the optimal pseudo-symbol sequence produced by the trellis demodulator becomes, as opposed to (12),

$$a_{0,n} = \begin{cases} j \cdot d_n; & n: \text{ even} \\ d_n; & n: \text{ odd} \end{cases}, \qquad a_{1,n} = \begin{cases} -d_n \cdot d_{n-1} \cdot d_{n-2}; & n: \text{ even} \\ -j \cdot d_n \cdot d_{n-1} \cdot d_{n-2}; & n: \text{ odd} \end{cases} \tag{17}$$

With the state still defined as $s_n=(d_n,d_{n-1})$, a 2^2-state 2^3-branch Viterbi algorithm is again sufficient for demodulating $\{d_n\}$ using $F=2$ matched-filters. The branch metric associated with the sign-alternating pre-coding scheme (16) is

$$l(n)=l(s_n,s_{n-1})=\begin{cases}\mathrm{Im}(r_{0,n})\cdot d_n-\mathrm{Re}(r_{1,n})\cdot d_n d_{n-1}d_{n-2}; & n:\ even\\ \mathrm{Re}(r_{0,n})\cdot d_n-\mathrm{Im}(r_{1,n})\cdot d_n d_{n-1}d_{n-2}; & n:\ odd\end{cases} \tag{18}$$

The choice between the pre-coding schemes (13) and (16) is, strictly speaking, quite arbitrary – the corresponding branch metric computations (15) and (18) involve only additions/subtractions of real quantities, and extensive simulations consistently yield identical demodulation performance for the two schemes. In the sequel, however, we opt for the sign-alternating scheme (16) on behalf of simplifying a serial demodulator which bases its data decision essentially on the sign of the first term in (18). [Serial demodulation is still feasible when using the pre-coding scheme (13) provided the modulo-4-related signs in the first term of (15) are properly accounted for in accordance with the modulo-4 conditions.]

The case of $F=4$ is sometimes of interest – particularly for GMSK signals with small BT-product such as $BT\le 1/6$. The additional two matched-filters and amended branch metrics for the $F=4$ case are

$$h_2(t)=h_0(t)\cdot\frac{c(t+2T_s)}{c(t-(L-2)T_s)},\quad h_3(t)=h_1(t)\cdot\frac{c(t+2T_s)}{c(t-(L-2)T_s)}$$
$$l(n)\equiv\mathrm{Re}\left[r_{0,n}\cdot a_{0,n}^{*}+r_{1,n}\cdot a_{1,n}^{*}+r_{2,n}\cdot a_{2,n}^{*}+r_{3,n}\cdot a_{3,n}^{*}\right] \tag{19}$$

With the pre-coding scheme (16) in place, the additional pseudo symbols are

$$a_{2,n}=\begin{cases}-j\cdot d_n d_{n-2}d_{n-3}; & n:\ even\\ -d_n d_{n-2}d_{n-3}; & n:\ odd\end{cases},\qquad a_{3,n}=\begin{cases}-d_n d_{n-1}d_{n-3}; & n:\ even\\ -jd_n d_{n-1}d_{n-3}; & n:\ odd\end{cases} \tag{20}$$

With the state now amended as $s_n=(d_n,d_{n-1},d_{n-2})$, it should be clear that a 2^3-state 2^4-branch Viterbi algorithm with the following branch metric is sufficient for demodulating $\{d_n\}$ using $F=4$:

$$l(n)=l(s_n,s_{n-1})=\begin{cases}\mathrm{Im}(r_{0,n})\cdot d_n-\mathrm{Re}(r_{1,n})\cdot d_n d_{n-1}d_{n-2}-\mathrm{Im}(r_{2,n})\cdot d_n d_{n-2}d_{n-3}-\mathrm{Re}(r_{3,n})\cdot d_n d_{n-1}d_{n-3}; & n:\ even\\ \mathrm{Re}(r_{0,n})\cdot d_n-\mathrm{Im}(r_{1,n})\cdot d_n d_{n-1}d_{n-2}-\mathrm{Re}(r_{2,n})\cdot d_n d_{n-2}d_{n-3}-\mathrm{Im}(r_{3,n})\cdot d_n d_{n-1}d_{n-3}; & n:\ odd\end{cases} \tag{21}$$

Figure A depicts a generic GMSK modem employing the data pre-coding scheme defined by either (13) or (16). The metric computation within the Viterbi algorithm is governed by the pre-coding scheme and the number F of matched filters used. Taking $a_n=d_n$ in the figure effectively removes data pre-coding.

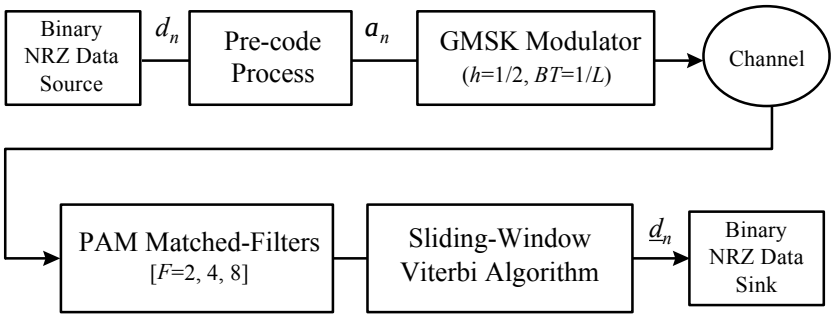

Figure A. Generic Binary GMSK Modem with Data Pre-code.

4. SIMULATION RESULTS

Performance Enhancement due to Data Pre-code

The performance enhancing effect of employing data pre-code is quantified in Figure 3 for BT∈ {1/2, 1/3, 1/4, 1/5}. The thick curves correspond to employing data pre-code (16), and thin curves correspond to no data pre-code. These simulation data show that, regardless of the BT value, a modem that employs data pre-code will, depending on the channel BER of interest, render a 0.5~1.5 dB signal-to-noise ratio (SNR) enhancement over the same modem that employs no data pre-code.

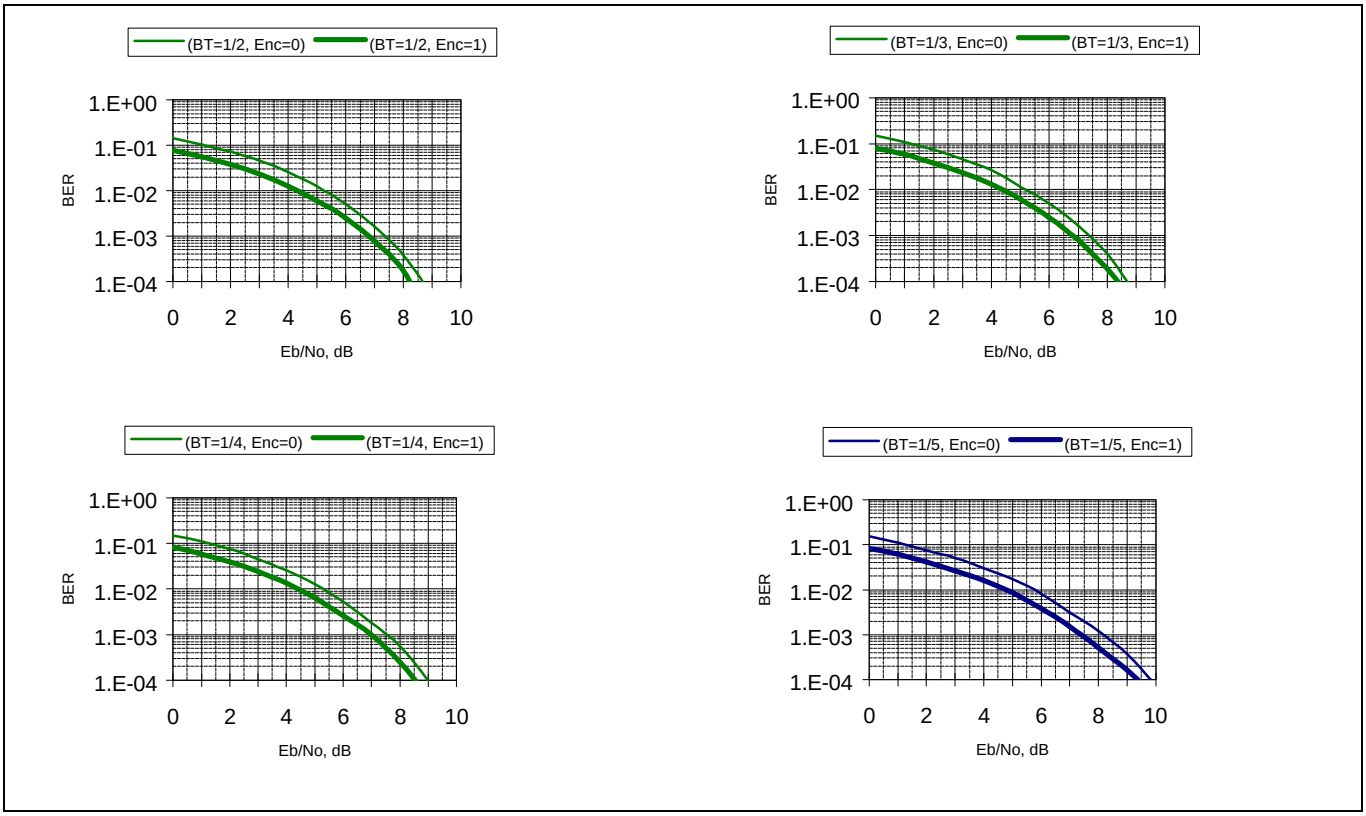

Figure 3. Performance Enhancement due to Data Pre-code.

Performance Dependency on BT

The performance of the (pre-coded) trellis demodulator in AWGN is depicted in Figure 4 for BT∈ {1/3, 1/4, 1/5, 1/6, 1/7}. Two matched-filters (F=2) are used here along with data pre-code (16). The SNR required for attaining any given channel BER is seen to be larger for smaller BT. Such a performance dependency on BT is intuitively anticipated: smaller BT yields longer signal memory L (along with narrower spectrum), hence severer inter-symbol-interference (ISI) in the signal. Note that, for BT=1/3, the 2-filter trellis demodulator already achieves the performance of coherent BPSK signaling.

Performance Dependency on Matched-filter Count *F*

The performance dependency on the number of matched-filters used in the trellis demodulator is quantified in Figure 5 for BT∈ {1/4, 1/5, 1/6, 1/7}. The performance of using F=2 and F=4 matched filters are compared with data pre-coded (16) in place. The solid curves correspond to F=2, and the dashed curves correspond to F=4. The performance benefit of using more matched-filters is seen quite significant for systems with small BT (e.g., BT≤1/6). This is particularly so for systems with low operating BER – such as those that do not employ forward-error-correction. On the other hand, regardless of the operating BER level, using F=2 matched-filters appears adequate for systems with large BT (e.g., BT≥1/5).

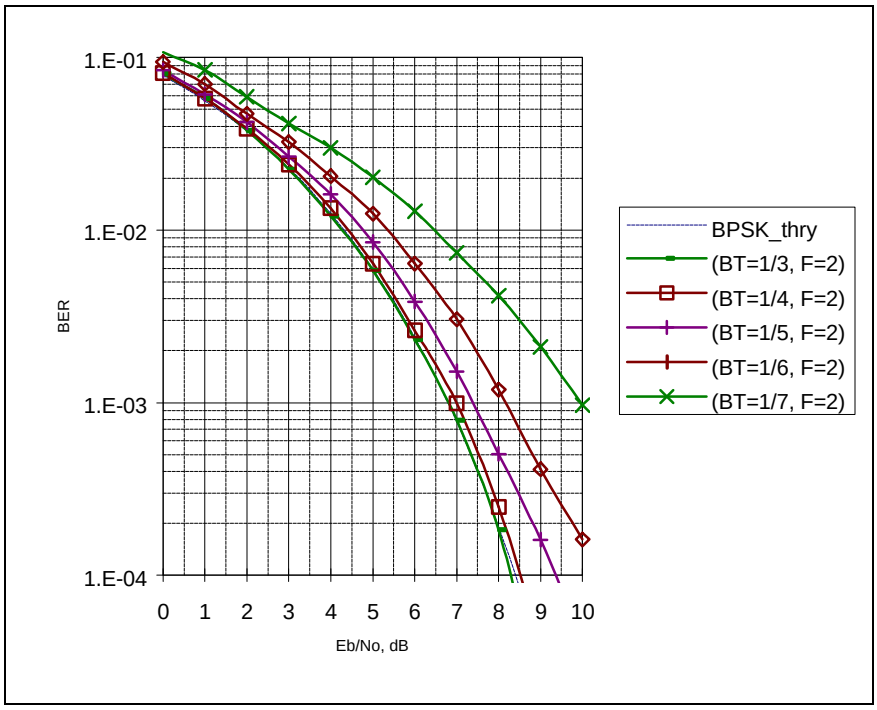

Figure 4. AWGN Performance of 2-filter Trellis Demodulator.

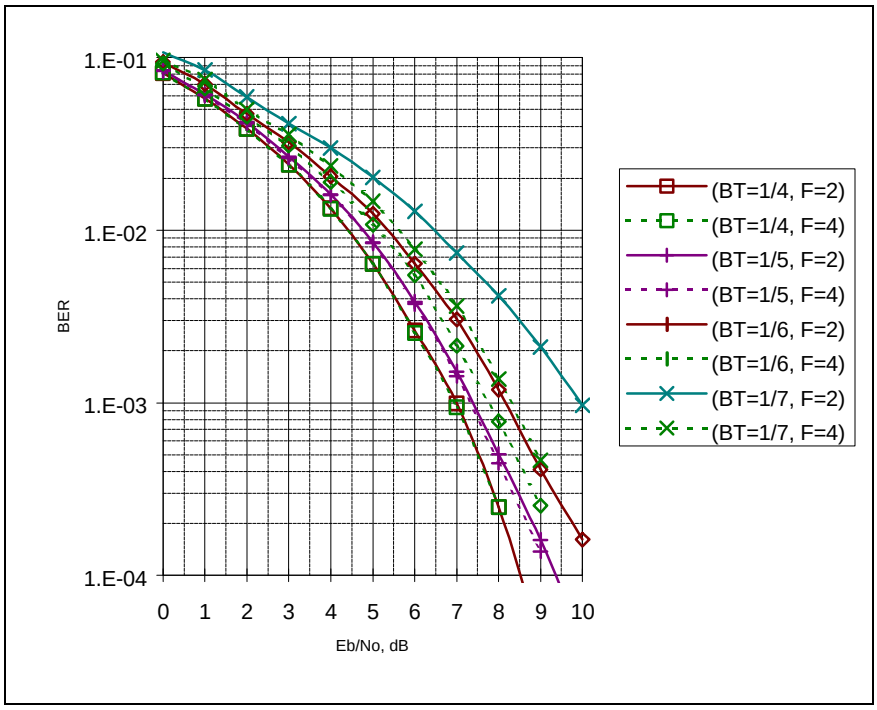

Figure 5. Performance Enhancement due to More Matched-Filters.

Performance in ACI

To assess the ACI performance of the (pre-coded) trellis demodulator we consider a typical FDMA scenario in which a desired GMSK signal is "surrounded" by two (identically modulated) interfering GMSK signals. Both interfering signals are equally separated from the desired signal in frequency (one on each side), and each has a power advantage of A_I dB over the desired signal. [The parameter A_I is used to account for the possible difference in propagation loss between the signals. It can also be used to reflect the worst-case power fluctuation between the signals.] The ACI performance using F=2 matched-filters and data pre-code (16) is depicted in Figure 6 and 7 where the SNR required to attain a 0.01 operating BER is plotted against the underlying carrier spacing for A_I=0 and 10 dB, respectively.

An intuitive power-versus-bandwidth tradeoff is evident in each of these curves: as multiple signals are packed closer and closer to achieve higher throughput, more and more power must eventually be exerted in order to maintain a given operating BER. Also evident in each curve is that there exists a *threshold carrier separation* below which no amount of power increase is enough to attain the given BER. Such threshold carrier separation is BT-dependent as well as A_I-dependent: smaller BT lowers the threshold, and larger A_I raises the threshold. These ACI simulation data also reveal a "threshold BT-product" as one pursues tighter carrier packing via using smaller BT. With A_I=0, for example, the threshold carrier separation is gradually lowered from $0.65R_b$ to $0.55R_b$ as BT decreases from 1/2 to 1/5, but decreasing BT below 1/5 will only lower the signal power efficiency without lowering such threshold. The threshold BT-product is thus 1/5. With

A_I=10 dB, the corresponding threshold BT-product occurs when BT=1/6 as the threshold carrier separation lowered from $0.85R_b$ to $0.65R_b$.

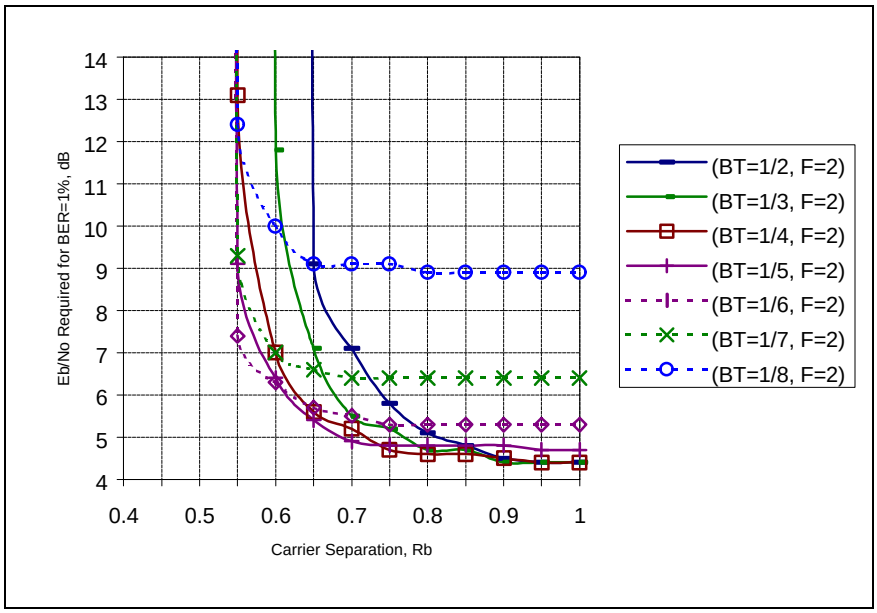

Figure 6. ACI Performance of 2-filter Trellis Demodulator A_I=0 dB.

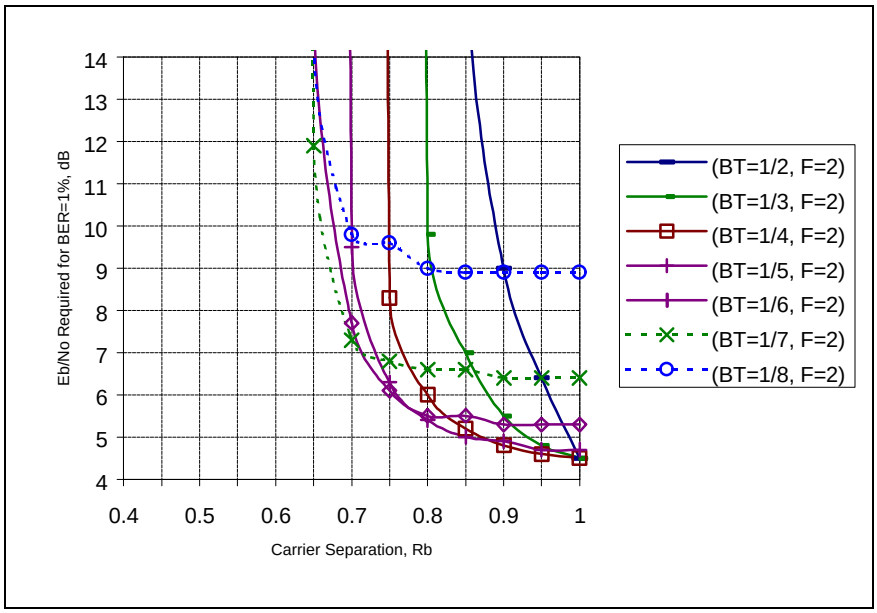

Figure 7. ACI Performance of 2-filter Trellis Demodulator A_I=10 dB.

CONCLUSIONS

The demodulation performance of binary GMSK signals for a wide range of BT using the PAM-based coherent trellis demodulator was presented. An easy-to-build, performance-enhancing, spectrum-preserving data pre-coding scheme has been devised and incorporated into the demodulator. Simulation data strongly support adopting data pre-

code for all values of BT. The performance dependency of the trellis demodulator on the number of PAM-based matched-filters was investigated. Simulation data indicate that F=4 matched-filters need only be considered for systems with small BT and/or low operating BER values. We have also quantified the ACI performance of the trellis demodulator under a typical FDMA interference scenario. Simulation data reveal a threshold BT-product in the presence of ACI. While the analytical PSD and in-band power ratio in Figures 1 and 2 allow one to quickly assess the spectral occupancy of binary GMSK signals, the ACI simulation results presented in Figures 6 and 7 provide a basis for a power-versus-bandwidth tradeoffs in using GMSK signals in an FDMA system.

REFERENCES

[1] G. Kaleh, "Simple Coherent Receivers for Partial Response Continuous Phase Modulation," IEEE *Journal On Selected Areas in Communications*, Vol. 7, No. 9, December, 1989.

[2] P. Laurent, "Exact Approximation Construction of Digital Phase Modulations by Superposition of Amplitude Modulated Pulses (PAM)," IEEE *Transactions on Communications*, Vol. 34, No. 2, February, 1986.

[3] J. Anderson, T. Aulin and C. Sundberg, *Digital Phase Modulation*, Plenum, New York, 1986.